



## Investigating the Effect of Parameters on the Dynamic Behavior of Permanent Magnet Stepper Motor Using State Space Analysis

Ghazanfar Shahgholian<sup>1,2</sup>, Majid Dehghani<sup>\*1,2</sup>, and Majid Moazami<sup>1,2</sup>

<sup>1</sup> Department of Electrical Engineering, Najafabad Branch, Islamic Azad University, Najafabad, Iran

<sup>2</sup> Smart Microgrid Research Center, Najafabad Branch, Islamic Azad University, Najafabad, Iran

Received: 08-Mar-2022, Revised: 15-Apr-2022, Accepted: 26-Apr-2022.

### Abstract

Stepping motors are normally operated without feedback and may suffer from loss of synchronization. The permanent magnet stepper motor (PMSM) is generally two-phase. In this paper, the nonlinear dynamic equations governing the performance of the permanent magnet stepper motor are linearized at an operating point for small signal stability studies. Small signal stability is the system ability to maintain synchronism when a small disturbance occurs. It is based on the state space averaging approach. A detailed description of the method, results, and conclusions are also presented. Finally, simulation results for three motors have been reported and compared.

**Keywords:** Eigenvalues Analysis, Linearized Model, Mode System, Permanent Magnet Stepper Motor, State Space.

### 1. INTRODUCTION

Considering the various applications of the machines, they are classified into three main types [1-14]: (a) machines generating mechanical energy (prime movers) such as: gas turbines, water turbines and steam engines, (b) machines transforming mechanical energy (converting machines) such as hydraulic pump and electric generator, (c) machines utilizing mechanical energy such as

lathe machine.

A stepper motor is an actuator that converts electrical pulses into angular displacement [2-19]. In recent years stepper motors are widely used in industries. Stepper motors are essentially incremental motion devices. A stepper motor is an electric machine that rotates in discrete angular increments. They can be used in both open and closed-loop modes, and are still the motor of choice in a wide range of applications. Stepper motors are mainly

---

\*Corresponding Authors Email:  
dehghani@pel.iaun.ac.ir

divided into three types: the permanent magnet motor, the variable reluctance motor, and the hybrid motor, which is a combination of the previous two [20,21]. The stepper motors have many advantages such as a) the rotation angle of the motor is proportional to the input pulse, b) a wide range of rotational speeds can be realized as the speed is proportional to the frequency of the input pulses and c) very reliable since there are no contact brushes in the motor. The main disadvantage of stepper motors is their reduced speed compared to servo motors and resonance if not properly controlled [22-25].

The operation of a PMSM is based on the repulsion or attraction between the rotor and the stator. Torque and volume are relatively small. The step angle is generally 7.5 or 15 degrees. The primary feature of the PMSM is that the rotor is made from permanent magnet, hence, no brush is needed. A PMSM is based on the relationship between stationary electromagnets and the permanent magnet rotor. A problem with this type of stepper motor is that it has limited torque and may only be used for low-speed applications. The cutaway diagram of a permanent magnet stepper motor is shown in Fig. 1. PMSM is essentially a low-cost, low-torque, low-speed device ideally suited to applications in fields such as computer peripherals. PM stepper motor has been extensively studied and used under open-loop operation. They are stable when they are operated as open loop system. These motors are widely used by industry for a variety of applications such as automotive control and driving the paper feed mechanism in line printers and printing terminals.

There are many publications describing

the various forms of stepper motors and methods by which they may be controlled [26,27]. The dynamic behavior of the rotor in a claw-poled PMSM is studied in [28], which the finite element method model of a prototype stepper is used to calculate the magnetic forces on the rotor. An approach to position control based on micro-stepping with comprises nonlinear torque modulation and a nonlinear current tracking controller for permanent magnet stepper motors is studied in [29]. An adaptive artificial neural network controller applies to PMSM for regulating its speed during the starting process under the full load torque and under load disturbance in [30], which is compared with the conventional PI controller.

A robust nonlinear position control for PMSMs is proposed in [31], where a single-output single-input model including position, speed, and acceleration is specified and it also has a reinforced observer designed to estimate position, speed, acceleration, and distortion.

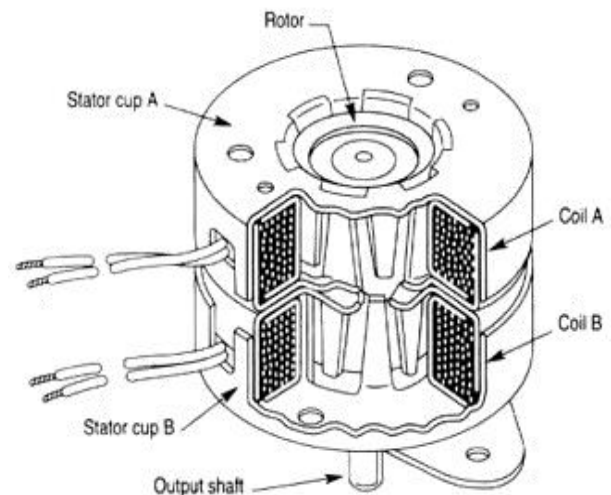


**Fig. 1. Cutaway diagram of a permanent magnet stepper motor.**

The PMSM is considered for use in high-performance positioning systems. PMSM is generally two-phase. In this paper, the nonlinear dynamics of a two-phase PMSM is studied by means of a linearized model. Analysis and simulation of small signal stability of PM stepper motor are presented. Mode space analysis has been used to investigate the effect of parameter changes on engine behavior. Section 2 presents the mathematical model of the PM stepper motor. Small signal stability analysis using linear techniques is shown in section 3. Simulation results are provided and discussed in Section 4. Finally, relevant conclusions are presented in section 5.

## 2. MATHEMATICAL MODELING

The mathematical model for PM stepper motor is highly nonlinear. This makes the design of a control procedure more difficult and justifies the use of linearization methods. A simplified schematic of a PM stepper motor that has a slotted stator with one pair and a PM rotor is shown in Fig. 2. The rotor in a PM stepper motor is a smooth cylindrical PM radially magnetized with alternating N and S poles. The stator has two cup-shaped halves with formed stator teeth [32].

In a PM stepper motor, four forms of energy are involved: electrical energy input, energy stored in the magnetic field coupling the stator and the rotor, energy converted to heat and mechanical energy output. The output torque and power from a stepper motor are functions of the motor size, motor heat sinking, working duty cycle, motor winding, and the type of driver used.

The dynamic behavior of the two-phase PM stepper motor is currently described in

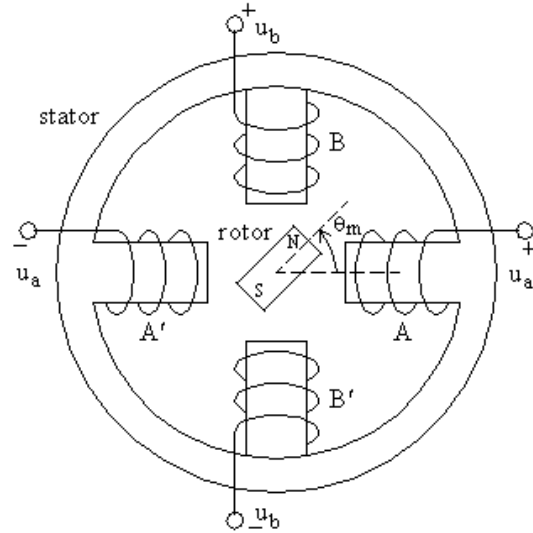


**Fig. 2. Schematic of a two-phase PM stepper motor.**

stationary two axes reference frame by the following set of electro-mechanical equations with four state variable and three inputs in the state space model [33]:

$$\frac{d}{dt}\theta_m = \omega_m = f_1(X) \quad (1)$$

$$\begin{aligned} \frac{d}{dt}\omega_m = \frac{1}{J}[-K_m i_a \sin(N_r \theta_m) + K_m i_b \cos(N_r \theta_m) \\ - B \omega_m - C \text{sign}(\omega_m) \\ - K_d \sin(4N_r \theta_m) - T_L] = f_2(X) \end{aligned} \quad (2)$$

$$\begin{aligned} \frac{d}{dt}i_a = \frac{1}{L}[u_a - R i_a + K_m \omega_m \sin(N_r \theta_m)] \\ = f_3(X) \end{aligned} \quad (3)$$

$$\begin{aligned} \frac{d}{dt}i_b = \frac{1}{L}[u_b - R i_b - K_m \omega_m \cos(N_r \theta_m)] \\ = f_4(X) \end{aligned} \quad (4)$$

where  $i_a$ ,  $i_b$  and  $u_a$ ,  $u_b$  are the currents and voltages in windings a and b, respectively.  $\omega_m$  is the angular velocity of the shaft of the motor,  $\theta_m$  is the angular displacement of the shaft of the motor,  $T_L$  is the unknown external

load torque. The parameters  $R$ ,  $L$ ,  $N_r$ ,  $J$ ,  $B$ , and  $C$  are constant and assumed to be perfectly known. The parameter  $C$ , for all analysis purposes, is assumed to be zero. The term  $T_T = K_d \sin(4N_r \theta_m)$  represents the detent torque due to the permanent rotor magnet interacting with the magnetic material of the stator poles. The  $\text{sign}(\omega_m)$  is defined as:

$$\text{sign}(\omega_m) = \begin{cases} \frac{\omega_m}{|\omega_m|} & \omega_m \neq 0 \\ 0 & \omega_m = 0 \end{cases} \quad (5)$$

The quadrature component  $i_q$  of the current produces torque while the direct component  $i_d$  does not produce any torque. A linear controller can then be used to control  $\omega_m$  using  $i_q$ .

A simple d-q coordinate state-space model of the two-phase PM stepper may be obtained by utilizing the d-q transformation:

$$\frac{d}{dt} \theta_m = \omega_m \quad (6)$$

$$\frac{d}{dt} \omega_m = \frac{1}{J_M} (K_m i_q - B \omega_m - T_L - C \text{sign}(\omega_m)) \quad (7)$$

$$\frac{d}{dt} i_d = \frac{1}{L} (u_d - R i_d + N_r L \omega_m i_q) \quad (8)$$

$$\frac{d}{dt} i_q = \frac{1}{L} (u_q - R i_q - N_r L \omega_m i_d - K_m \omega_m) \quad (9)$$

where  $i_d$  is the direct current,  $i_q$  is the quadrature current,  $u_d$  is the direct voltage and  $u_q$  is the quadrature voltage. The quadrature component of the current ( $i_q$ ) produces torque while the direct component  $i_d$  does not produce any torque. A linear controller can then be used to control  $\omega_m$  using  $i_q$ .

Generally, the torque of the stepper motor

at low speed is close to the holding torque. Since the output torque reduces with the increase of speed and the output power changes with the increase of speed as well, the holding torque becomes one of the most important parameters of measuring stepper motors.

### 3. STABILITY ANALYSIS

The transfer function of a system represents the relationship describing the dynamics of the system under consideration. The dynamic equations governing the performance of the PM stepper motor are nonlinear. They are linearized about an operating point for small signal stability studies.

Small signal stability analysis using linear techniques provides valuable information about the inherent dynamic characteristics of the PMSM and assists in its design. For small signal stability, the linearized system model is acceptable.

The dynamic equations governing the performance of the PM stepper motor given in (1) to (4) are nonlinear. They are linearized about an operating point ( $U_{ao}$ ,  $U_{bo}$ ,  $T_{Lo}$ ,  $\omega_{mo}$ ,  $\theta_{mo}$ ,  $I_{ao}$ ,  $I_{bo}$ ) for small signal stability studies and assist in its design.

By linearizing about an output point, the total linearized PMSM model can be represented by the following equation:

$$\frac{d}{dt} \Delta X = A \Delta X + B \Delta U \quad (10)$$

$$\Delta Y = C \Delta X + D \Delta U \quad (11)$$

where  $\Delta X$  is the state vector,  $\Delta Y$  is the output vector,  $\Delta U$  is the input vector,  $A$  is the state matrix,  $B$  is the control or input matrix,  $C$  is the output matrix and  $D$  is the feed forward

matrix. The elements of matrix A and B are:

$$a_{ik} = \left. \frac{\partial f_i}{\partial x_k} \right|_{X_o} \quad (12)$$

$$b_{ik} = \left. \frac{\partial f_i}{\partial u_k} \right|_{X_o} \quad (13)$$

Therefore, the linearized equations of the system are given by:

$$\frac{d}{dt} \Delta\theta_m = \Delta\omega_m \quad (14)$$

$$\begin{aligned} \frac{d}{dt} \Delta\omega_m = & \frac{-K_m N_r [I_{ao} \cos(N_r \theta_{mo}) + I_{bo} \sin(N_r \theta_{mo})]}{J} \Delta\theta_m \\ & - \frac{K_m \sin(N_r \theta_{mo})}{J} \Delta i_a + \frac{K_m \cos(N_r \theta_{mo})}{J} \Delta i_b \\ & \frac{4 K_d N_r \cos(4 N_r \theta_{mo})}{J} \Delta\theta_m - \frac{B}{J} \Delta\omega_m - \frac{1}{J} \Delta T_L \end{aligned} \quad (15)$$

$$\begin{aligned} \frac{d}{dt} \Delta i_a = & \frac{1}{L} \Delta u_a - \frac{R}{L} \Delta i_a + \frac{K_m \sin(N_r \theta_{mo})}{L} \Delta\omega_m \\ & + \frac{K_m N_r \omega_{mo} \cos(N_r \theta_{mo})}{L} \Delta\theta_m \end{aligned} \quad (16)$$

$$\begin{aligned} \frac{d}{dt} \Delta i_b = & \frac{1}{L} \Delta u_b - \frac{R}{L} \Delta i_b - \frac{K_m \cos(N_r \theta_{mo})}{L} \Delta\omega_m \\ & + \frac{K_m \omega_{mo} N_r \sin(N_r \theta_{mo})}{L} \Delta\theta_m \end{aligned} \quad (17)$$

In this section, the stability characteristics are determined by examining the eigenvalues of the A matrix.

The block diagram of the system is depicted in Fig. 3, in which constant gain is given by:

$$K_A = K_m \sin(N_r \theta_{mo}) \quad (18)$$

$$K_B = K_m \cos(N_r \theta_{mo}) \quad (19)$$

$$\begin{aligned} K_M = & -N_r (K_A I_{ao} + K_B I_{bo}) \\ & - \frac{4 K_d N_r}{J} \cos(4 N_r \theta_{mo}) \end{aligned} \quad (20)$$

In this model the magnetic material is assumed to be linear, i.e, the effect of saturation at high currents is neglected, also the model hysteresis and eddy currents are assumed negligible.

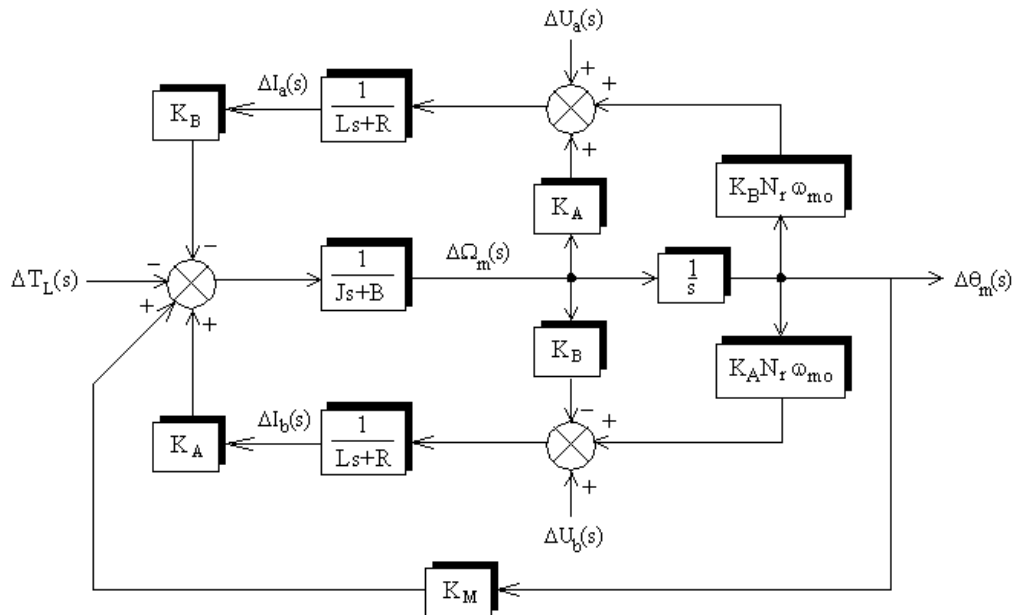


Fig. 3. Open loop block diagram of the system.

**Table 1. The Parameters of Various Motors.**

parameter	motor A	motor B	motor C	unit
$N_r$	50	50	50	-
$L$	1.1	1	4.6	mH
$R$	10	8.4	0.28	$\Omega$
$K_m$	0.113	0.05	0.464	Nm/A
$K_d$	0.0339	0	0.12	Nm
$J$	$5.7 \times 10^{-6}$	$3.6 \times 10^{-6}$	$3.65 \times 10^{-4}$	kg.m <sup>2</sup>
$B$	$1 \times 10^{-3}$	$1 \times 10^{-4}$	$11 \times 10^{-3}$	N.m.s/r

**Table 2. Eigenvalues for three PM stepper motors.**

A	B	C
-550	-500	-360
-464	-481	-253
$-43.7 \pm j514.0$	$-10.2 \pm j243.7$	$-68.8 \pm j557.3$
$\eta = 0.0847$	$\eta = 0.0418$	$\eta = 0.1225$
$\omega_n = 516.1$	$\omega_n = 244.6$	$\omega_n = 561.5$
$T_s = 0.0686$	$T_s = 0.2941$	$T_s = 0.0436$

The transfer function that relates the mechanical angular velocity to the voltage and torque is given by:

$$\Omega_m(s) = H_{MA}(s)\Delta U_a(s) + H_{MB}(s)\Delta U_b(s) + H_{ML}(s)\Delta T_L(s) \quad (21)$$

where:

$$H_{MA}(s) = \frac{-K_B s}{\Delta(s)} \quad (22)$$

$$H_{MB}(s) = \frac{K_A s}{\Delta(s)} \quad (23)$$

$$H_{ML}(s) = \frac{-(Ls + R)s}{\Delta(s)} \quad (24)$$

The characteristic equation is:

$$\Delta(s) = s^4 + \underbrace{\frac{2RJ + LB}{LJ}}_{a_3} s^3 + \underbrace{\frac{JR^2 + RB(L+1) + 2K_A^2 K_B^2 - K_M L}{LJ}}_{a_2} s^2 + \underbrace{\frac{R(RB + K_A^2 + K_B^2)}{L^2 J}}_{a_1} s + \underbrace{\frac{-K_M R^2}{L^2 J}}_{a_0} \quad (25)$$

A necessary condition for stability of the system is that all the roots in characteristic equation have a negative real part, which in turn requires that all coefficients ( $a_3$ ,  $a_2$ ,  $a_1$ ,  $a_0$ ) are positive. The coefficients depend on the parameters of the motor and they don't depend on the initial conditions and input changes. Therefore, there are four eigenvalues for PM stepper motor that one of the roots is  $s_1 = -R/L$ . Typically the characteristic equations of control system are high order and transfer function poles are classified into 1) dominant poles which are effective on dynamic behavior of the system and 2) unimportant poles.

#### 4. SIMULATION RESULTS

The dynamic analysis is verified by transfer

function simulation using MATLAB and time domain simulation of the PMSM. Table 1 shows the fundamental parameters of the PM stepper motor used in digital computer simulation with MATLAB to verify the performance of the proposed analysis scheme. The eigenvalues open loop linearized system, damping ratio ( $\eta$ ), and undamped natural frequency ( $\omega_n$ ) of the second order system for various motors are summarized in Table 2. The settling time ( $T_s$ ) can be approximated using  $\eta$  and  $\omega_n$ . The current of two phase winding in terms of time is shown in Figs. 4 and 5. The mechanical angular velocity and mechanical rotor angle in terms of time is shown in Figs. 6 and 7. Fig. 8 shows the mechanical angular velocity in terms of mechanical rotor angle.

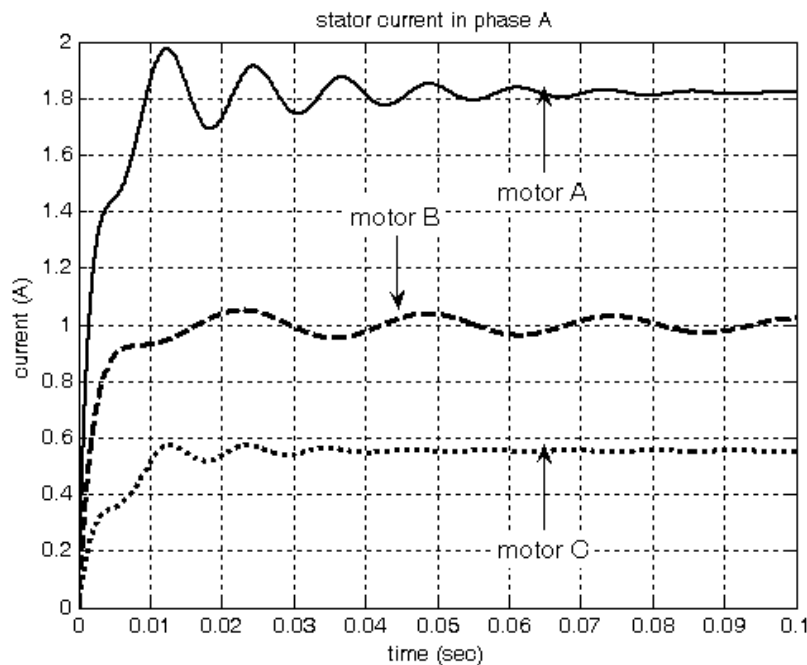


**Fig. 4. Plot of current of phase A.**

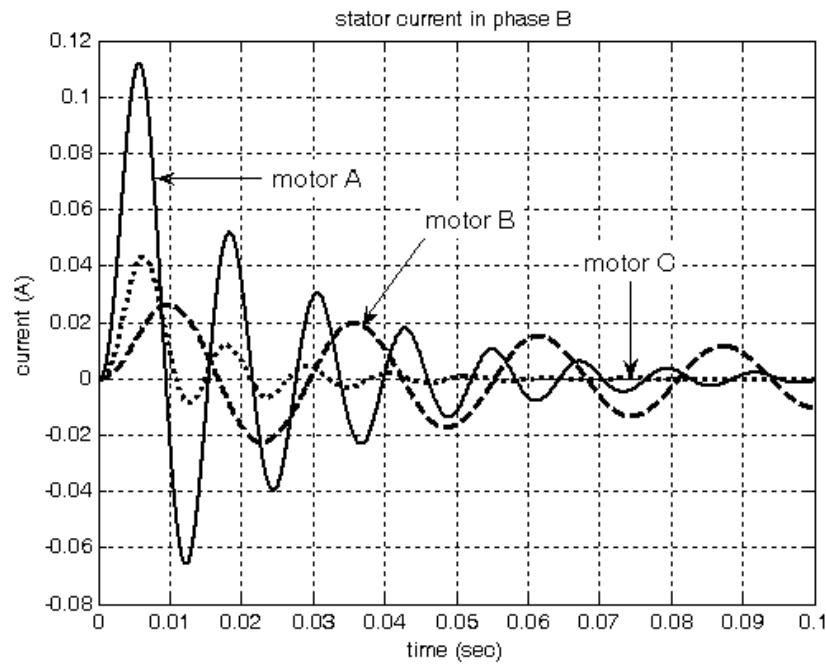


**Fig. 5.** Plot of current of phase B.

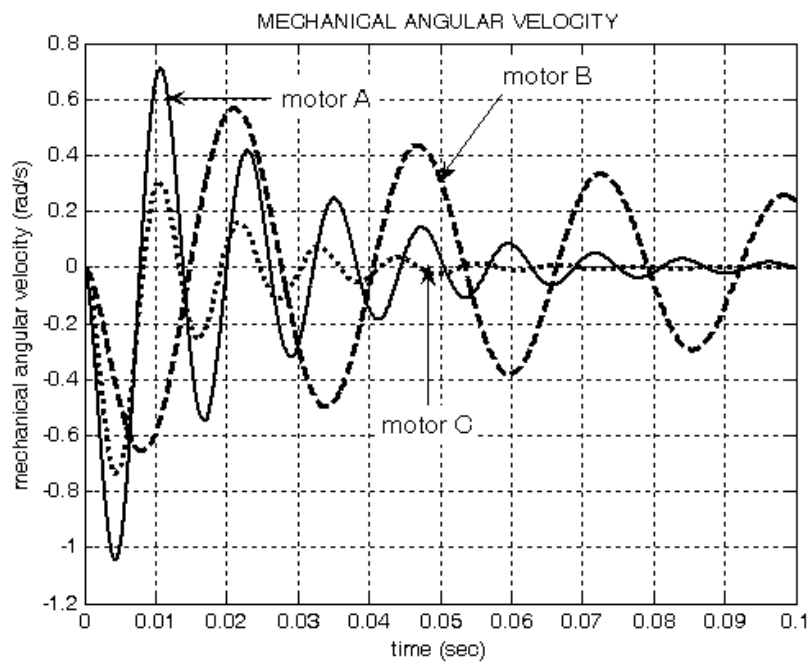


**Fig. 6.** Plot of mechanical angular velocity in terms of time.

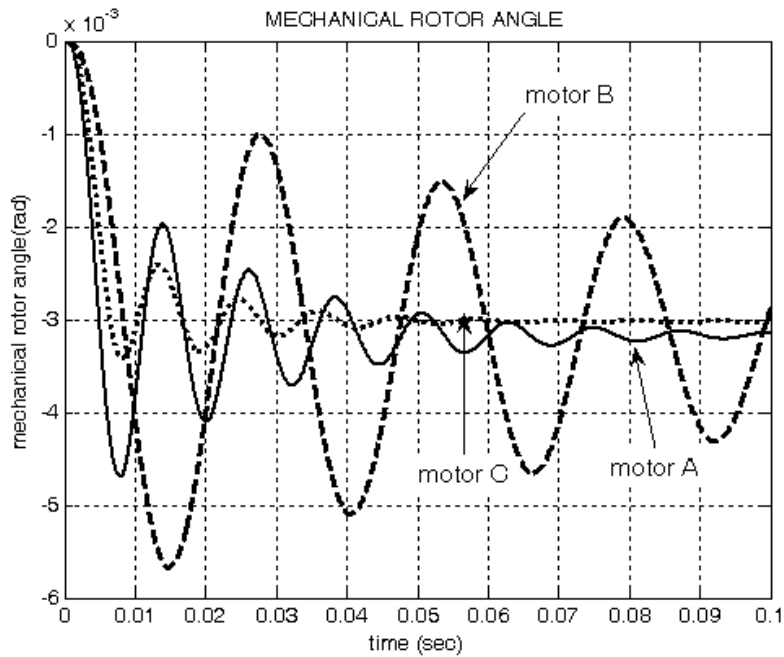


**Fig. 7. Plot of mechanical rotor angle in terms of time.**

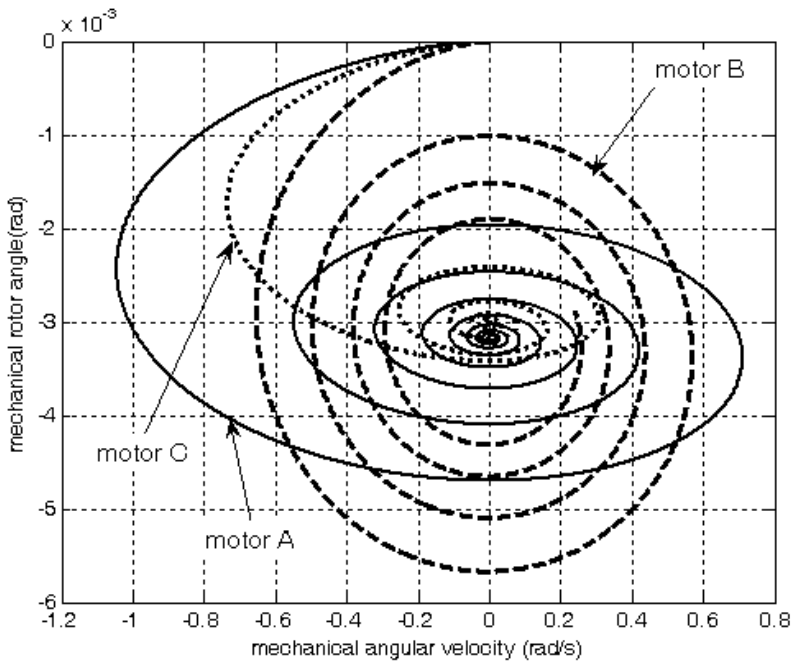


**Fig. 8. Plot of mechanical angular velocity and mechanical rotor angle.**

Linearized models are useful for control system tuning using linear analysis techniques such as frequency response. The frequency response of the open loop system

phase a current and mechanical angular velocity are shown in Figs. 9 and 10, respectively.

The model represented by (1) to (4), neglects the slight magnetic coupling between the phases, small magnetic coupling between the phase windings, small change in inductance as a function of rotor position, the detent torque, and variation in inductance due

to magnetic saturation, i.e., assumes negligible air gap variations.

In this section, a comparative study of different parameters of the PM stepper motor is shown. The dynamic performances of the PM stepper motor are analyzed, for three different resistance and inductance.

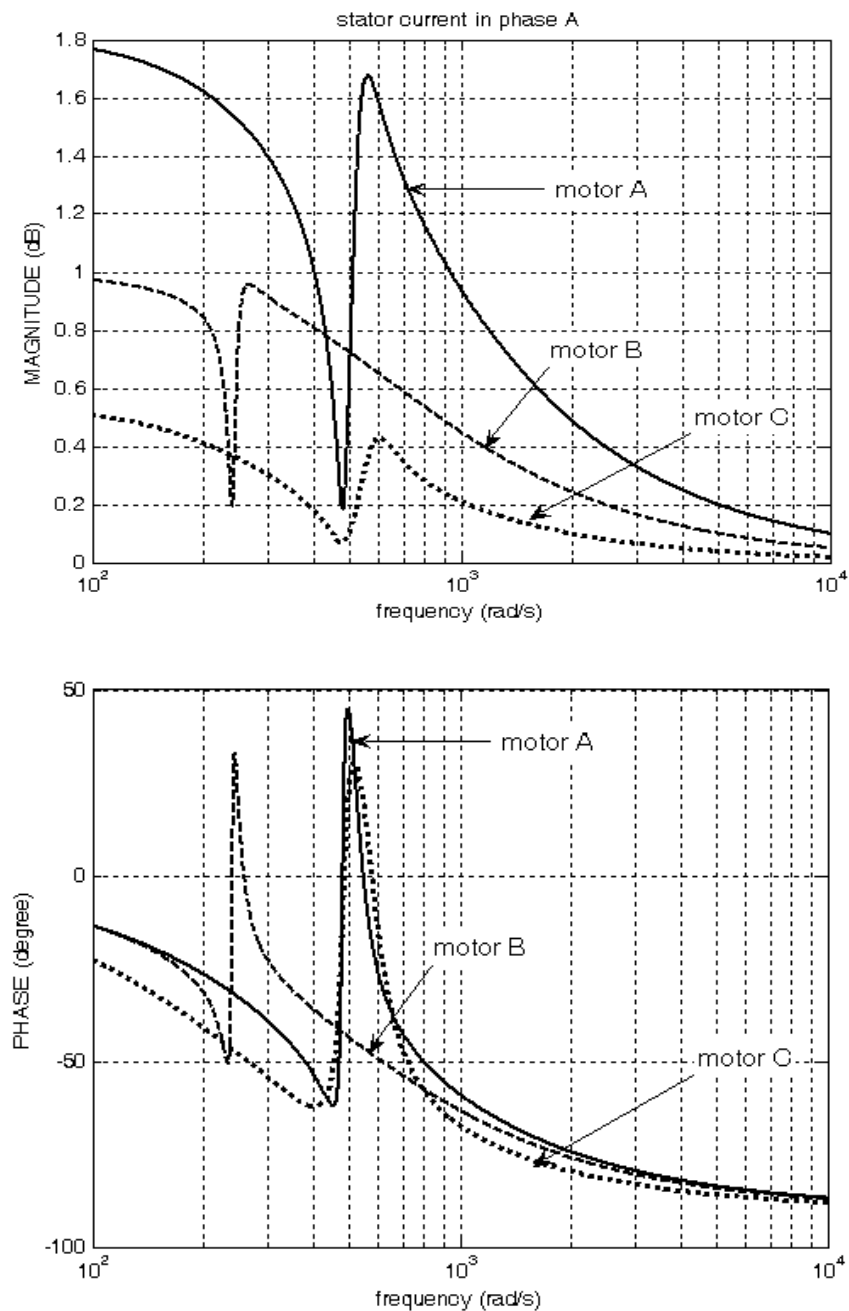


**Fig. 9.** Frequency characteristic of the open loop system of current of phase A.

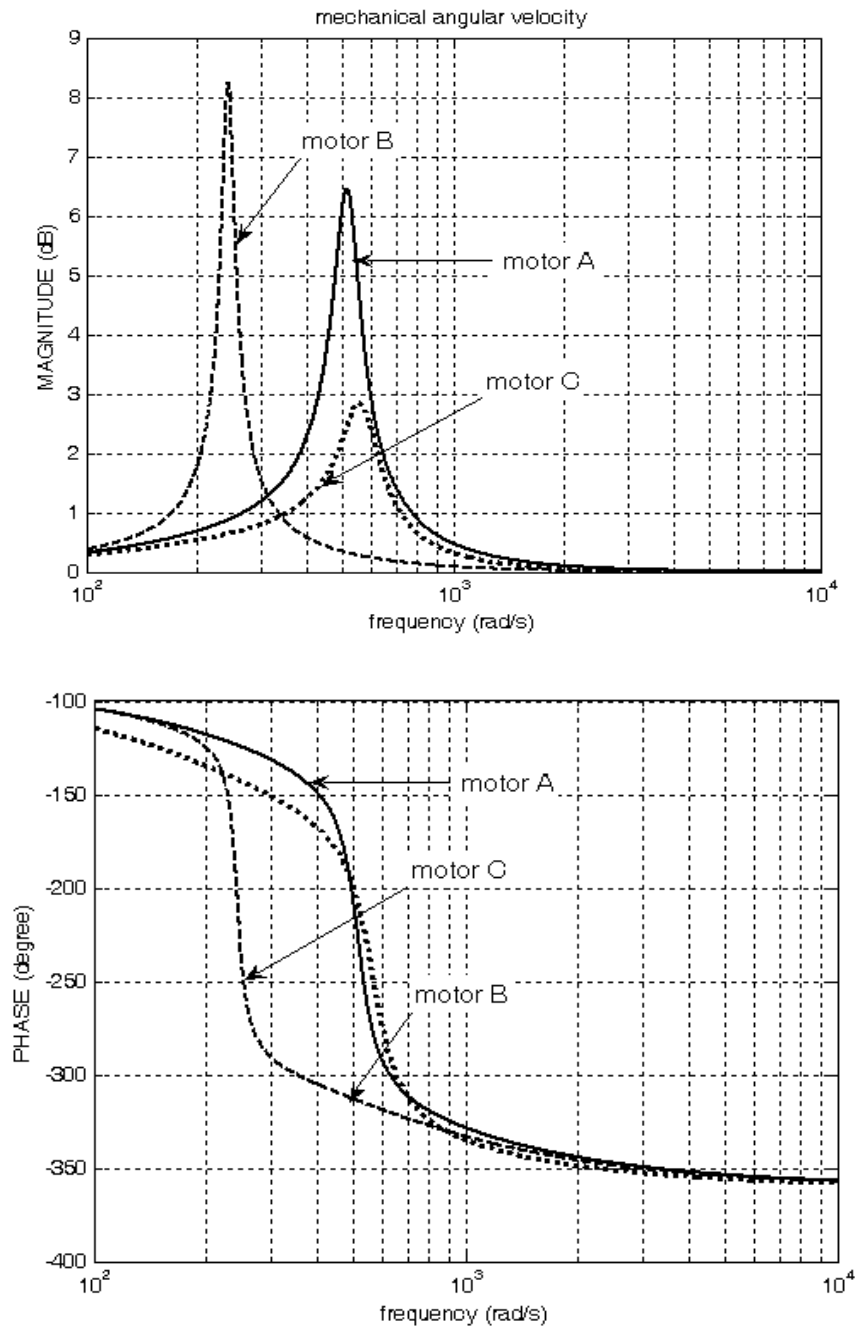


**Fig. 10.** Frequency characteristic of the open loop system of mechanical angular velocity.

The eigenvalues of the open loop linearized system for various parameters are summarized in Tables 3 and 4.

An increase in the motor resistance decreases the natural frequency and increases the settling time. Conversely, increasing the

motor inductance decreases both the natural frequency and the damping ratio, but increases the settling time. The step response with different resistance and inductance are presented in Figs. 11, and 12, and Figs. 13, and 14, respectively.

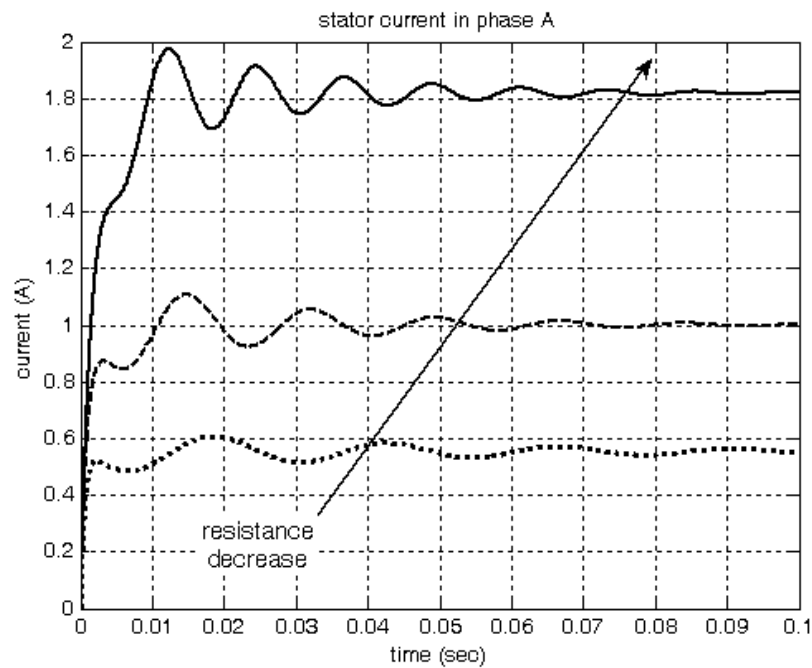


**Fig. 11.** Plot of current of phase A for different resistance of motor A.

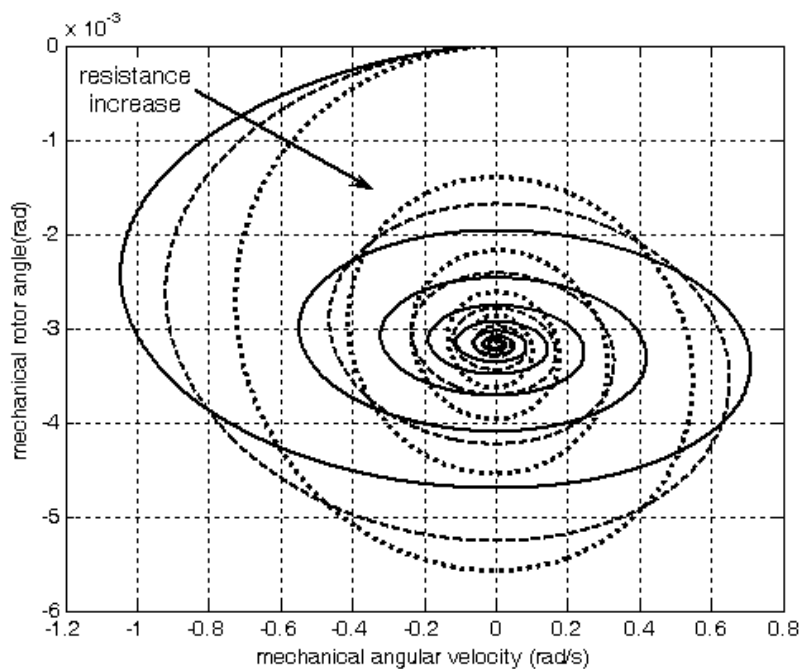


**Fig. 12.** Plot of mechanical angular velocity and mechanical rotor angle different resistance of motor A.

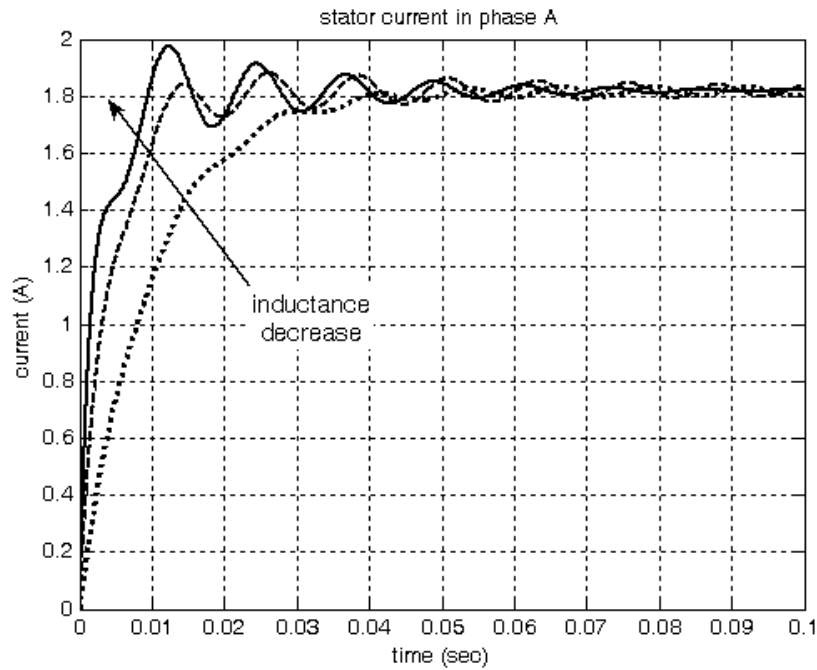


Fig. 13. Plot of current of phase A for different inductance of motor A.

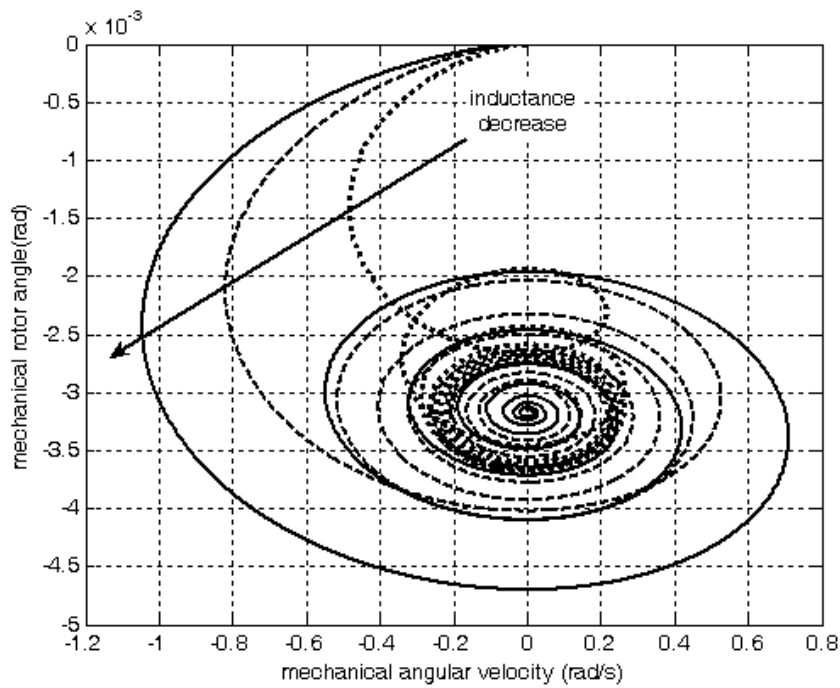


Fig. 14. Plot of mechanical angular velocity and mechanical rotor angle different inductance of motor A.

**Table 3. Eigenvalues for different resistance of motor A.**

<b>R=0.55</b>	<b>R=1.00</b>	<b>R=1.80</b>
-550	-1000	-1800
-464	-923	-175
$-43.7 \pm j514.0$	$-39.3 \pm j363.2$	$-23.5 \pm j261.8$
$\eta = 0.0847$	$\eta = 0.1076$	$\eta = 0.0894$
$\omega_n = 516.1$	$\omega_n = 365.3$	$\omega_n = 16.2$
$T_s=0.0686$	$T_s=0.0763$	$T_s=0.1277$

**Table 4. Eigenvalues for different inductance of motor A.**

<b>L=0.001</b>	<b>L=0.002</b>	<b>L=0.005</b>
-550	-275	-110
-464	-240	-103
$-43.7 \pm j514.0$	$-18.2 \pm j506.5$	$-4.4 \pm j490.0$
$\eta = 0.0847$	$\eta = 0.0359$	$\eta = 0.009$
$\omega_n = 516.1$	$\omega_n = 506.8$	$\omega_n = 490.0$
$T_s=0.0686$	$T_s=0.1648$	$T_s=0.6818$

## 5. CONCLUSION

Stepping motors are robust and very reliable. To select the power equipment, drive, and control design, it is necessary to study the PM stepper motor performance using the linearization technique. The aim of this paper is to simulate the dynamic small signal behavior of a PM stepper motor. Finally, by linearizing the nonlinear differential equations of the motor, simulation results for three motors have been reported and discussed.

## REFERENCES

[1] H. Farnaghizad, H. lesani, "Optimal

design of an axial flux PMSM for hybrid vehicle use", Signal Processing and Renewable Energy, Vol. 2, No. 2, pp. 25-29, 2018.

- [2] A. Ahmadpour, S. Seyed Shenava, A. Dejamkhooy, E. Mokaramian, "Electromagnetic force analysis of transformer on the ferroresonance due to consecutive 3-phase short-circuit faults using finite element method (FEM)", Journal of Intelligent Procedures in Electrical Technology, Vol. 11, No. 41, pp. 47-60, June 2020.
- [3] G. Shahgholian, J. Faiz, N. Sedri, P. Shafaghi, M. Mahdavian, "Design and experimental analysis of a high speed two-phase induction motor drive for

- weaver machines applications", International Review of Electrical Engineering, Vol. 5, No. 2, pp. 454-461, April 2010.
- [4] S. Zhang, C. Wang, H. Zhang, P. Ma, X. Li, "Dynamic analysis and bursting oscillation control of fractional-order permanent magnet synchronous motor system", Chaos, Solitons & Fractals, Vol. 156, Article Number: 111809, 2022.
- [5] S. Samadinasab, F. Namdari, M. Bakhshipoor, "A novel approach for earthing system design using finite element method", Journal of Intelligent Procedures in Electrical Technology, vol. 8, no. 29, pp. 54-63, June 2017.
- [6] X. Wang, S. Lu, S. Zhang, "Rotating angle estimation for hybrid stepper motors with application to bearing fault diagnosis", IEEE Trans. on Instrumentation and Measurement, Vol. 69, No. 8, pp. 5556-5568, Aug. 2020.
- [7] J. Choi and M. S. Illindala, "Effect of prime mover's characteristics on the survivability of a synchronous generator-based distributed energy resource during transient overload conditions", IEEE Trans. on Industry Applications, vol. 56, no. 1, pp. 88-94, Jan.-Feb. 2020.
- [8] S. Saberian Borojeni, "Fuzzy second order sliding mode speed observer for a synchronous reluctance motor with predictive control", Journal of Intelligent Procedures in Electrical Technology, Vol. 4, No. 13, pp. 45-52, 2013.
- [9] R. Cao, Y. Jin, M. Lu, Z. Zhang, "Quantitative comparison of linear flux-switching permanent magnet motor with linear induction motor for electromagnetic launch system", IEEE Trans. on Industrial Electronics, Vol. 65, No. 9, pp. 7569-7578, Sept. 2018.
- [10] W. Liu, H. Yang, H. Lin, L. Qin, "Hybrid analytical modeling of air-gap magnetic field in asymmetric-stator-pole flux reversal permanent magnet machine considering slotting effect", IEEE Trans. on Industrial Electronics, vol. 69, no. 2, pp. 1739-1749, Feb. 2022.
- [11] D. Jang, H. Shin, S. Paul, J. Chang, Y. Yun, "Design of a high-force electro-mechanical actuator for electrically driven lathe machine", IEEE Trans. on Industrial Electronics, Vol. 67, No. 11, pp. 9526-9535, Nov. 2020.
- [12] M. Jafarboland, A. Nekoobin, "Designing a two-phase BLDC motor and finite-element analysis of stator slots structure effects on the motor operation", Journal of Intelligent Procedures in Electrical Technology, Vol. 5, No. 17, pp. 15-20, Spring 2014.
- [13] Y.H. Wang, Y.H. Liu, Y.R. Yang, R.Y. Wang, "Effects of square-stepping exercise on motor and cognitive function in older adults— A systematic review and meta-analysis", Geriatric Nursing, Vol. 42, No. 6, pp. 1583-1593, 2021.
- [14] G. Shahgholian, M. Maghsoodi, "Analysis and simulation of speed control in DC motor drive by using fuzzy control based on model reference adaptive control", Cumhuriyet Science

- Journal, Vol. 37, No. 3, pp. 197-211, Oct. 2016.
- [15] J. Pillans, "Reducing position errors by vibration optimization of stepper motor drive waveforms", *IEEE Trans. on Industrial Electronics*, vol. 68, no. 6, pp. 5176-5183, June 2021.
- [16] G.S. Gupta, P.R. Tripathi, S. Kumar, S. Ghosh, R.K. Sinha, "Prototype design for bidirectional control of stepper motor using features of brain signals and soft computing tools", *Biomedical Signal Processing and Control*, Vol. 71, Article Number: 103245, 2022.
- [17] J. Faiz, G. Shahgholian, H. Ghazizadeh, "Analysis of dynamic behavior of switched reluctance motor-design parameters effects", *Proceeding of the IEEE/MELCON*, pp. 532-537, Valletta, Malta, April 2010.
- [18] M. Hojati, A. Baktash, "Hybrid stepper motor with two rows of teeth on a cup-shaped rotor and a two-part stator", *Precision Engineering*, Vol. 73, pp. 228-233, 2022.
- [19] M. Bodson, J.N. Chiasson, R.T. Novotnak, R.B. Rekowski, "High-performance nonlinear feedback control of a permanent magnet stepper motor", *IEEE Trans. on Control Systems Technology*, Vol. 1, No. 1, pp. 5-14, March 1993.
- [20] B. Lu, Y. Xu, X. Ma, "Design and analysis of a novel stator-permanent-magnet hybrid stepping motor", *IEEE Trans. on Applied Superconductivity*, Vol. 26, No. 7, Oct. 2016.
- [21] S. Derammelaere, B. Vervisch, J.D. Viaene, K. Stockman, "Sensorless load angle control for two-phase hybrid stepper motors", *Mechatronics*, Vol. 43, pp. 6-17, May 2017.
- [22] A.M. Harb, A.A. Zaher, "Nonlinear control of permanent magnet stepper motors", *Communications in Nonlinear Science and Numerical Simulation*, Vol. 9, No. 4, pp. 443-458, 2004.
- [23] H. Fukumoto, T. Yamaguchi, M. Ishibashi, T. Furukawa, "Developing a remote laboratory system of stepper motor for learning support", *IEEE Trans. on Education*, vol. 64, no. 3, pp. 292-298, Aug. 2021.
- [24] J.E. Vadell, L.E. Chiang, "Stepping motor driving by controlled-energy discharge", *IEEE Trans. on Industrial Electronics*, vol. 46, no. 1, pp. 52-60, Feb. 1999.
- [25] Y. -L. Huang, C. -H. Liang, B. -H. Chen and C. -C. Lan, "Torque-sensorless control of stepper motors for low-cost compliant motion generation", *IEEE Access*, vol. 9, pp. 94495-94504, 2021.
- [26] W. Kim, C.C. Chung, "Novel position detection method for permanent magnet stepper motors using only current feedback", *IEEE Trans. on Magnetic*, Vol. 47, No. 10, pp. 3590-3593, Oct. 2011.
- [27] J. Hong, S. Wang, Y. Sun, H. Cao, "An effective method with copper ring for vibration reduction in permanent magnet brush dc motors", *IEEE Trans. on Magnetics*, Vol. 54, No. 11, pp. 1-5, Nov. 2018.
- [28] J. Ārkofic, M. Boltežar, "Numerical modelling of the rotor movement in a permanent-magnet stepper motor", *IET Electric Power Applications*, Vol. 8, No. 4, pp. 155-163, April 2014.

- 
- [29] W. Kim, D. Shin, C.C. Chung, "Microstepping with nonlinear torque modulation for permanent magnet stepper motors", *IEEE Trans. on Control Systems Technology*, Vol. 21, No. 5, pp. 1971-1979, Sep. 2013.
- [30] H.M. Hasanién, "FPGA implementation of adaptive ANN controller for speed regulation of permanent magnet stepper motor drives", *Energy Conversion and Management*, Vol. 52, No. 2, pp.1252–1257, Feb. 2011.
- [31] W. Kim, Y. Lee, D. Shin, C.C. Chung, "Nonlinear Gain Position Control Using Only Position Feedback for Permanent Magnet Stepper Motors", *IEEE Trans. on Power Electronics*, Vol. 36, No. 7, pp. 8506-8516, July 2021.
- [32] H. Sira-Ramírez, "A passivity plus fleness controller for the permanent magnet stepper motor", *Asian Journal of Control*, Vol. 2, No. 1, pp. 1-9, Mar. 2000.
- [33] E.N. Sanchez, A.G. Loukianov, R.A. Felix, "Dynamic triangular neural controller for stepper motor trajectory tracking", *IEEE Trans. on Systems, Man, and Cybernetics*, Vol. 32, No. 1, pp. 24-30, Feb. 2002.